

Proceedings of the

Advanced Architectures in Photonics

September 21–24, 2014

Prague, Czech Republic

Volume 1

Editors

Jiri Orava

University of Cambridge
Department of Materials Science and Metallurgy
27 Charles Babbage Road
CB3 0FS Cambridge
United Kingdom

Tohoku University
WPI-Advanced Institute for Materials Research
(WPI-AIMR)
2-1-1 Katahira, Aoba-ku
980-8577 Sendai
Japan

Tomas Kohoutek

Involved Ltd.
Siroka 1
537 01 Chrudim
Czech Republic

Proceeding of the Advanced Architectures in Photonics
<http://aap-conference.com/aap-proceedings>

ISSN: 2336-6036
September 2014

Published by **Involved Ltd.**
Address: Siroka 1, 53701, Chrudim, Czech Republic
Email: info@involved.cz, Tel. +420 732 974 096



This work is licensed under a
[Creative Commons Attribution
3.0 Unported License](https://creativecommons.org/licenses/by/3.0/).

CONTENTS

[Preface](#)

T. Wagner (Chairman)	i
----------------------------	---

FULL PAPERS

[Innovative nanoimprint lithography](#)

S. Matsui, H. Hiroshima, Y. Hirai and M. Nakagawa	1
---	---

[Nanofabrication by imprint lithography and its application to photonic devices](#)

Y. Sugimoto, B. Choi, M. Iwanaga, N. Ikeda, H. T. Miyazaki and K. Sakoda	5
--	---

[Soft-mould imprinting of chalcogenide glasses](#)

T. Kohoutek, J. Orava and H. Fudouzi	9
--	---

[Electric nanoimprint to oxide glass containing alkali metal ions](#)

T. Misawa, N. Ikutame, H. Kaiju and J. Nishii	11
---	----

[Producing coloured materials with amorphous arrays of black and white colloidal particles](#)

Y. Takeoka, S. Yoshioka, A. Takano, S. Arai, N. Khanin, H. Nishihara, M. Teshima, Y. Ohtsuka and T. Seki	13
--	----

[Stimuli-responsive colloidal crystal films](#)

C. G. Schafer, S. Heidt, D. Scheid and M. Gallei	15
--	----

[Opal photonic crystal films as smart materials for sensing applications](#)

H. Fudouzi and T. Sawada	19
--------------------------------	----

[Introduction of new laboratory device 4SPIN® for nanotechnologies](#)

M. Pokorny, J. Rebíček, J. Klémes and V. Velebný	20
--	----

[Controlling the morphology of ZnO nanostructures grown by Au-catalyzed chemical vapor deposition and chemical bath deposition methods](#)

K. Govatsi and S. N. Yannopoulos	22
--	----

[Visible photon up-conversion in glassy \$\(\text{Ge}_{25}\text{Ga}_{5}\text{Sb}_{5}\text{S}_{65}\)_{100-x}\text{Er}_x\$ chalcogenides](#)

L. Strizik, J. Zhang, T. Wagner, J. Oswald, C. Liu and J. Heo	27
---	----

POSTERS presented at AAP 2014

[Solution processing of As-S chalcogenide glasses](#)

T. Kohoutek	31
-------------------	----

[Ga-Ge-Sb-S:Er³⁺ amorphous chalcogenides: Photoluminescence and photon up-conversion](#)

L. Strizik, J. Oswald, T. Wagner, J. Zhang, B. M. Walsh and J. Heo	32
--	----

[Multi-wavelength and multi-intensity illumination of the GeSbS virgin film](#)

P. Knotek, M. Kincl and L. Tichý	33
--	----

[Towards functional advanced materials based using filling or ordered anodic oxides supports and templates](#)

J. M. Macak, T. Kohoutek, J. Kolar and T. Wagner	34
--	----

[Introduction of new laboratory device 4SPIN® for nanotechnologies](#)

M. Pokorny, J. Rebíček, J. Klémes and V. Velebný	35
--	----

[Profile and material characterization of sine-like surface relief Ni gratings by spectroscopic ellipsometry](#)

J. Mistrik, R. Antos, M. Karlovec, K. Palka, Mir. Vlcek and Mil. Vlcek	36
--	----

[Preparation of sparse periodic plasmonic arrays by multiple-beam interference lithography](#)

M. Vala and J. Homola	37
-----------------------------	----

[High-performance biosensing on random arrays of gold nanoparticles](#)

B. Spackova, H. Sipova, N. S. Lynn, P. Lebruskova, M. Vala, J. Slaby and J. Homola	38
--	----

Controlling the morphology of ZnO nanostructures grown by Au-catalyzed chemical vapor deposition and chemical bath deposition methods

K. Govatsi and S. N. Yannopoulos*

Foundation for Research and Technology - Hellas, Institute of Chemical Engineering Sciences, (FORTH/ICE-HT), P.O. Box 1414, GR-26504, Rio-Patras, Greece

*Electronic mail: sny@iceht.forth.gr

One-dimensional nanostructures, e.g. nanowires, nanorods, nanotubes and so on, are emerging materials in nanoscience and nanotechnology due to their exceptional physical properties and their potential for a wide range of applications in optoelectronic and nanophotonic devices. High temperature thermal evaporation and solution chemistry approaches are the main synthetic routes. Controlled growth affects the morphology of nanowire arrays which ultimately dictate their optical and electrical properties. We briefly present methods for the controlled growth of ZnO nanowires by both approaches.

Nanomaterials or nanostructured materials are usually classified into three categories depending on their shape, i.e. zero-dimensional (0D), one-dimensional (1D) and two-dimensional (2D). Quantum dots and nanowires/nanorods are typically used to describe 0D and 1D materials, respectively [1]. Quantum dots are perhaps the most common example of semiconductor nanostructures confined in all three dimensions; their hallmark is the tunability of their optical properties used for *in vivo* imaging and diagnostics [2]. However, over the last two decades, another important class of 1D semiconductor nanostructures aroused considerable interest. Such structures have cross-sections in the range 10–100 nm and lengths extending to several micrometers. Although the term “nanowiskers” was originally used [3] to describe the growth of ultrafine InAs whiskers with diameters less than 20 nm on GaAs substrates, the term nanowires (NWs) has prevailed [4]. The merit of these anisotropic nanosized objects is that confinement – with its availing consequences in the material’s properties – occurs only in two dimensions while the third micrometer-sized dimension makes the manipulation of NWs in technological applications feasible. The long dimension also provides a pathway for the fast and lossless transport of electrons, holes and photons, rendering NWs favorable candidates for micro/nano-electronics and nano-photonics.

As mentioned above, NWs combine spatial confinement effects in 2D with the ability of feasible manipulation (long dimension). The majority of the current investigations concerning applications of NWs pertain to the field of renewable energy sources and in particular to solar energy harvesting and conversion. In this context, the unique electrical and optical properties of NWs render these 1D objects important energy conversion materials with applications in solar and photo-electrochemical cells.

Perhaps, the major advantages of NWs are the integrity and qualities of their structure. Their single-crystalline nature ensures very small defect density and the absence of other structural irregularities within the NW. In addition, the growth of NWs is not only limited to semiconducting oxides. A wide class of materials, including superconductors, metals, insulators, semiconductors and so on, can be produced as NWs. Rational growth methods have been developed allowing today the fabrication of arrays/assemblies of nanowires of various geometries and orientations as shown in Fig. 1. Oriented NWs perpendicular (vertical, Fig. 1a) and parallel (in-plane, Fig. 1b) to the substrate, as well as meshes of ordered NWs can be fabricated, which depending on the aspect ratio of NWs and the pitch of the array, provide tunable physical properties, such as optical, electrical, magnetic, and so on. More complex nanostructures, called nanoforests, have been envisaged to provide enhancement of the surface area, in comparison to simple NWs, where hierarchical growth results in tree-like morphologies, as illustrated in Fig. 2. Such hierarchical structures have been shown to result in a five-fold increase of the solar cell efficiency compared to simple upstanding ZnO NWs [5]. The efficiency increase was assigned to the enhanced surface area, which made higher dye loading and light harvesting possible. In addition, the branched geometry offers direct conduction pathways resulting in the reduction of charge recombination.

A major concern in the comparison between NW arrays and nanoparticle thin films relates to the surface area of the active material which is a key parameter for dye absorption in dye-sensitized solar

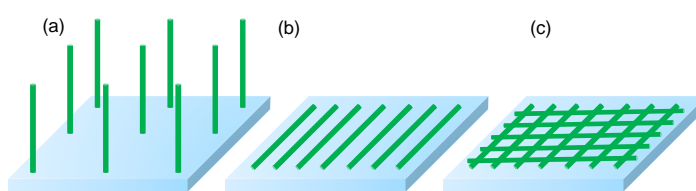


Figure 1. Arrays of NWs: (a) Vertical growth, (b) in-plane growth, (c) ordered mesh of in-plane grown NWs.

cells. Nanoparticle films are considered to provide a few times higher surface area in comparison to NW arrays. Low temperature, simple and cost-effective chemistry has demonstrated that dense arrays, up to 35 billion wires per cm^2 , can be grown on arbitrary substrates of any size [6]. The schematic shown in Fig. 3 reveals that the side surface of a nanowire of length L and diameter D , $S_{\text{NW}} = \pi D L$ is equal the surface of an arrangement of an arrangement of nanospheres occupying the same volume, i.e. $S_{\text{sp}} = \pi D^2 * L/D = \pi D L$, where L/D stands for the number of spheres over a length equal of L . This shows that the surface area of a dense array of well-aligned NWs can approach or even surpass the surface area of equally order arrays of spheres of the same diameter.

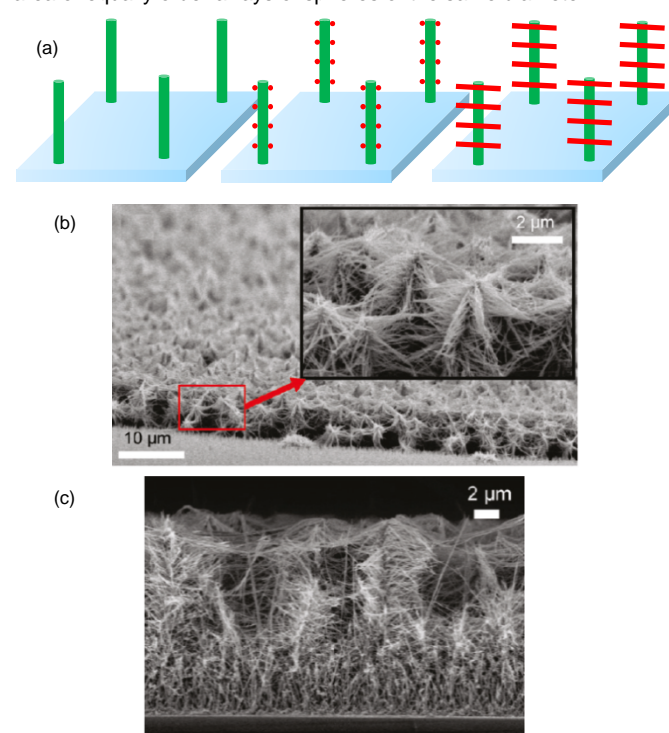


Figure 2. (a) Schematic illustration of the growth of branched NWs. Scanning electron microscopy images of branched NWs: tilted view (b) and cross section (c); adapted with permission from Ref. [5], copyright (2011) American Chemical Society.

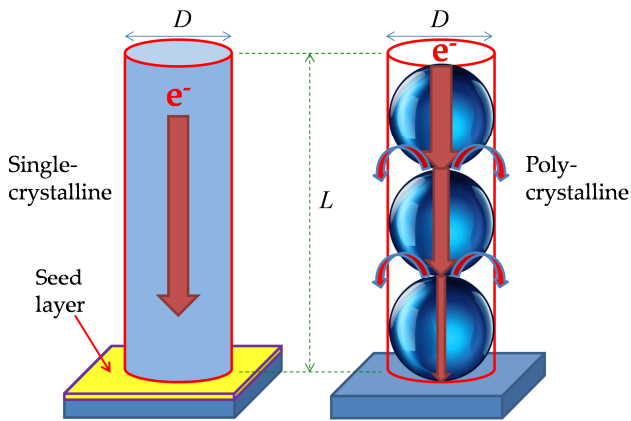


Figure 3. Schematic representations of the electron transport in a photoanode based on single-crystalline NWs and nanoparticles.

Closing this section, it is worth mentioning that NW films exhibit better mechanical properties than their nanoparticles-based counterparts. The solution growth process involving the growth from a seed layer ensures also a much stronger attachment to the substrate in the case of NW arrays.

Polymorphism of ZnO Nanostructures

According to Wang [7] there are three main types of 1D nanostructures that are being actively studied in nanotechnology: carbon nanotubes, silicon NWs, and ZnO NWs. ZnO, a wide bandgap semiconductor (3.37 eV) having a high electron-hole binding energy (60 meV), is an important transparent material [8]. ZnO exhibits a dazzling variety of nanostructure configurations (Fig. 4) [9], thus having a wide range of applications in optics, optoelectronics, spintronics, sensors, actuators, the energy sector, biomedical sciences, etc. ZnO nanocrystals are non-toxic, biosafe, and their large-scale production does not present environmental and health hazards [10]. Early work on semiconductor nanowhiskers [3] was followed by systematic studies in the area of inorganic NWs [11]. In the late 1990s, the field of semiconductor NWs underwent a significant expansion and became one of the most active research areas in nanoscience [12]. A boost in the study of ZnO nanostructures was given by the discovery of ZnO nanobelts [13] and the demonstration of ultra-violet lasing properties of ZnO NWs at room temperature [14]. These two articles [13, 14] have been the most influential in the development of the research focused on ZnO nanostructures. In brief, the latest representative breakthroughs in the field of ZnO nanostructures include:

- The development of the first examples of logic gates based on ZnO NW arrays which can be switched simply by bending the substrate, exploiting the piezotronic effect [15]. Using only ZnO NWs, the first piezoelectric triggered mechanical-electronic logic operation using the piezotronic effect was demonstrated.
- The realization of self-powered ZnO NW devices [16]. It was shown that the vertical and lateral integration of ZnO nanowires into arrays are capable of producing sufficient power to operate real devices. A lateral integration of 700 rows of ZnO NWs could produce a peak voltage of 1.26 V at a low strain of 0.19%, which is potentially sufficient to recharge an AA battery.
- The fabrication of optical fiber/ZnO-NW hybrid structures for efficient 3D dye-sensitized solar cells (DSSC) [17]. The ZnO NWs were grown normal to the optical fiber surface in order to enhance the surface area for the interaction of light with dye molecules. In this arrangement, the light illuminates the fiber from one end along the axial direction, and its internal reflection within the fiber creates multiple opportunities for energy conversion at the interfaces.
- The use of aligned ZnO-NWs in photovoltaic devices [6]. The authors introduced a version of the DSSC in which the traditional nanoparticle film was replaced by a dense array of oriented, crystalline ZnO nanowires, facilitating the rapid collection of carriers generated throughout the device. Later, ZnO NWs grown hydrothermally into nanoforest formations have yielded energy conversion efficiencies up to 2.6% [5].

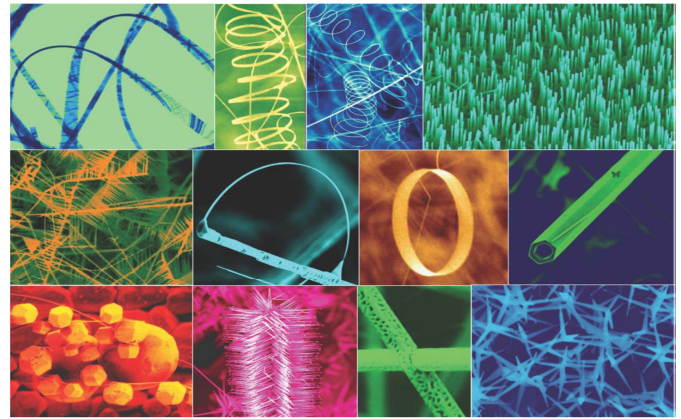


Figure 4. Typical morphologies of ZnO nanostructures grown under controlled conditions by thermal evaporation of solid powders. Adapted with permission from Ref. [9].

- The doping of ZnO nanorods with transition metal ions in order to fabricate diluted magnetic semiconductors with intrinsic ferromagnetism offering great potential in spintronics [18].

Synthesis of ZnO nanowires

A large number of physical and chemical methods have been applied for the growth of ZnO NWs. The majority of the approaches make use of bottom-up synthetic routes offering the possibility for a controlled growth of NWs with the desired aspect ratio, areal density and positional order on the substrate, enabling also the possibility for heterostructure growth. ZnO nanowires can be either grown as free standing particles in a solution or on specific substrates. As has been discussed in the previous sections, the aligned vertical-to-the-substrate growth of NWs entails certain advantages for energy conversion as well for photonic applications. The wurtzite structure of ZnO has two essential features, i.e. the non-central symmetry and the polar surfaces. The atomic arrangement in ZnO is described as a number of alternating planes composed of tetrahedrally coordinated Zn^{2+} and O^{2-} ions, stacked successively along the c-axis. The unit cell of ZnO is neutral; however, the ion distribution is such that some surfaces can be terminated entirely with cations or anions, resulting in positively or negatively charged surfaces, the so-called polar surfaces. The basal plane is the most common polar surface. Zn-(0001) and the O-(000-1) are the positively and negatively polar surfaces, respectively. These polar surfaces result in a normal dipole moment and a spontaneous polarization along the c-axis. Energetic reasons for maintaining a stable structure demand that the polar surfaces have facets or undergo considerable surface reconstructions. Below, we focus on two techniques most commonly employed for nanowire growth: chemical vapor deposition (CVD) and solution phase growth (or chemical bath deposition).

Chemical vapor deposition of ZnO nanowires

In the CVD method, chemical precursors are introduced as vapors into the hot zone of a furnace. Their reaction (mainly) onto a substrate heated at a selected temperature often takes place in the presence of a nanostructured metal catalyst which has been predeposited on the substrate. Vapor-liquid-solid (VLS) and the vapor-solid-solid (VSS) are the two main mechanisms for the growth of ZnO NWs. In the VLS mechanism a metal catalyst (in the form of nanoparticles) forms a liquid eutectic with the desired nanowire material [19]. The gaseous reactants dissolve progressively into the liquid eutectic droplet, which leads to a supersaturated solution facilitating nucleation and growth. The nucleated material precipitates; continuous feeding of the liquid catalyst droplet leads to further precipitation and nanowire growth. The VLS method is quite flexible allowing the growth of heterostructures by changing the source reactants. Nanowires with superlattice arrangements can be grown by the periodic introduction of different reactants. Furthermore, selecting appropriate experimental conditions, epitaxial layers on the side walls can also grow. In general, both axial and radial heterostructures can be synthesized by VLS. The first demonstration of ZnO NWs growth with perfect vertical alignment to the substrate (single crystalline sapphire) was achieved by Huang *et al.* [14] where the NWs array was shown to exhibit room-temperature ultraviolet lasing.

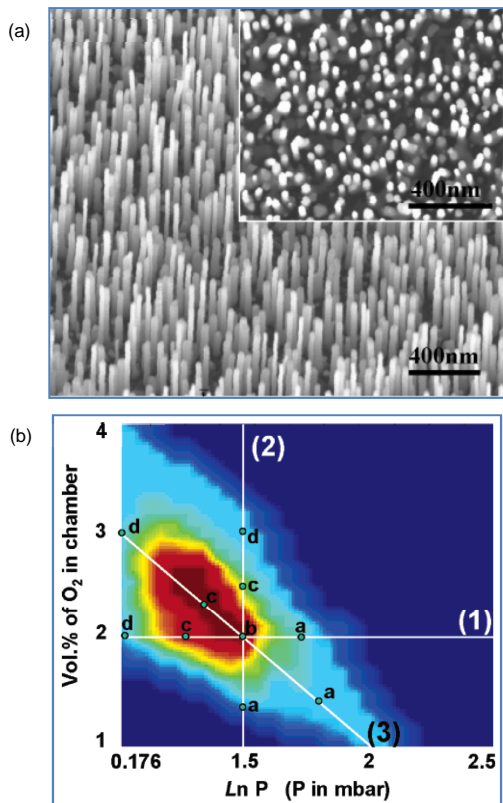
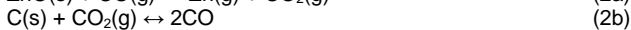
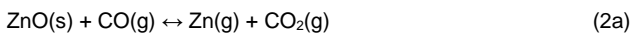


Figure 5. (a) SEM images of aligned ZnO nanorods on a GaN substrate. (b) “Phase diagram” correlating the O₂ partial pressure and the growth chamber pressure. Lines (1), (2), and (3) represent growth with constant O₂ pressure, constant system pressure, and linearly varying O₂ percentage and system pressure. Adapted with permission from Ref. [21], copyright (2005) American Chemical Society.

The growth of well-aligned ZnO NWs requires a rather low growth rate. Since the ZnO sublimation temperature (~1300 °C) is quite high, an alternative method to provide the reactants for ZnO growth is to adopt the carbothermal reduction by mixing ZnO and carbon powders. In this case, the reaction temperature can be reduced to 900 °C. The overall reaction (reduction) of ZnO can be written as:



The main intermediate reactions are the:



The zinc can be fully or partially oxidized in the air stream leading to the formation of stoichiometric ZnO or suboxides (ZnO_x, x<1). Both Zn and ZnO_x are volatile; after being transferred by an inert gas they reach the substrate. Since reaction (1) is reversible at somewhat lower temperatures than the carbothermal reduction, the vapors merge in the Au liquid droplet and react to form ZnO. The alignment of the ZnO NWs depends to a large extent on the epitaxial relationship between ZnO and the substrate. The very small lattice mismatch between ZnO and various materials has made it possible to produce well aligned ZnO NWs on sapphire [14] and various nitrides (GaN, AlGaN, AlN) [20].

Although the VLS growth mechanism is considered as one of the simplest methods for NW growth, a number of externally controlled experimental parameters render this method quite inextricable. In particular, the reaction temperature, the temperature gradient (between the source and the substrate), the growth time, the vapor pressure of Zn or ZnO, the inert gas and oxygen partial pressures, the gas concentration and flow rate, the type of the substrate, and the catalyst details (predominantly Au films deposited by sputtering and annealed to form NPs) are among the parameters that should be optimized for a controlled growth of ZnO NWs. The chamber total pressure, the oxygen partial pressure and the thickness of catalyst layer are the most important parameters.

An exhaustive investigation of the influence of the oxygen partial pressure and the chamber pressure on the quality and growth

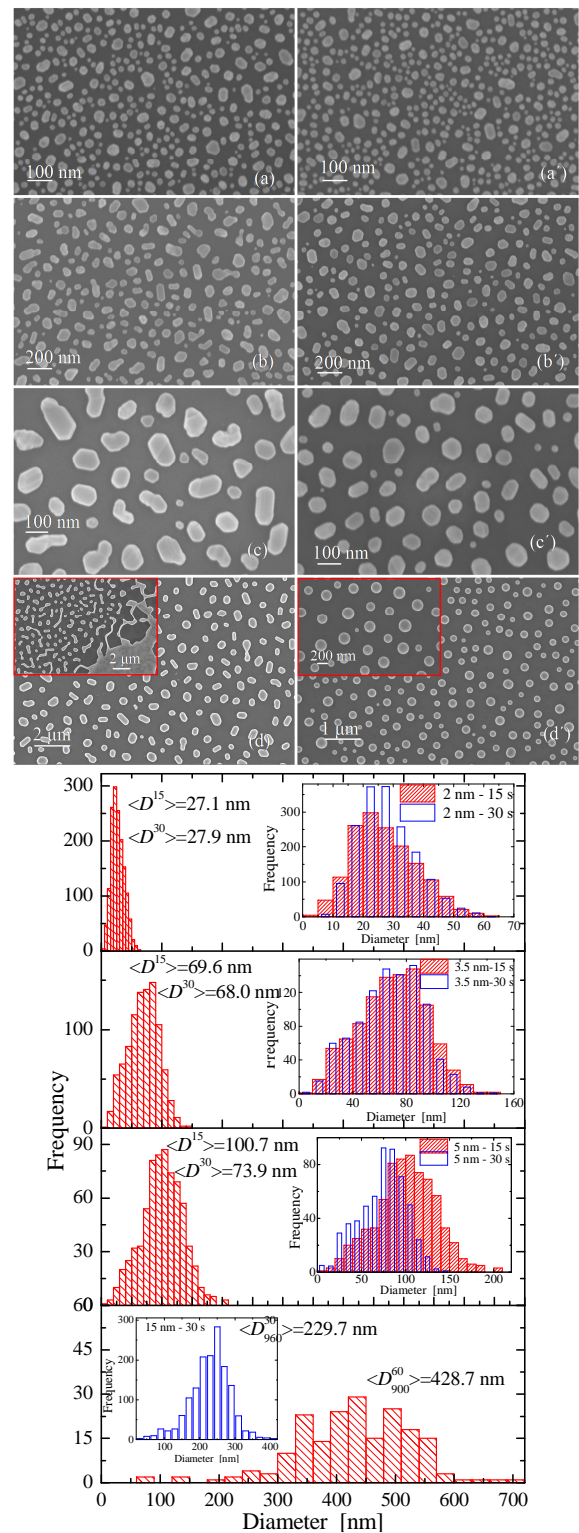


Figure 6. Top panel: SEM images of dewetted Au films. Nominal Au film thickness, annealing temperature and time are as follows: (a) 2 nm, 900 °C, 15 s; (a') 2 nm, 900 °C, 30 s; (b) 3.5 nm, 900 °C, 15 s; (b') 3.5 nm, 900 °C, 30 s; (c) 5 nm, 900 °C, 15 s; (c') 5 nm, 900 °C, 30 s; (d) 15 nm, 900 °C, 60 s (inset: 15 nm, 900 °C, 30 s); (d') 15 nm, 960 °C, 30 s (inset: magnification). Bottom panel: Particle size distributions of the Au nanoparticles shown in the left panel. The insets show the comparison between the PSDs obtained for the two different annealing times. Adapted with permission from Ref. [23].

behavior of ZnO NWs has been presented by Song et al. [21]. Conducting more than 100 experiments under different growth conditions, a quantitative definition of the best combination of the O₂ partial pressure and the chamber pressure for growing well-aligned ZnO NWs was achieved (Fig. 5(a)). The results were used to construct a kind of “phase diagram” of the controlled NW growth as shown in Fig. 5(b). Dark red regions represent the best growth conditions in terms of NWs with perfect alignment, high areal density

and uniform length and diameter. No growth of ZnO NWs was detected in the dark blue region.

The thickness of the catalyst layer that is pre-deposited on the substrate plays a dominant role for the morphology of the NWs. It is a general perception that the size of the catalyst particles determines the width of nanowires. However, it was shown that this condition is practically valid as long as the catalyst nanoparticle sizes do not exceed 40 nm [22]. While Au is the most frequently used catalyst for growing ZnO nanowires, its morphological features on the substrate, which determine the size and shape of the nanostructures grown, were not put into focus until recently. In a recent detailed study [23] we investigated the details of the solid state thermal dewetting of Au films into nanoparticles on Si substrates. Au films of various thicknesses ranging from 2 to 15 nm were annealed with slow and fast rates at various temperatures, and the morphological details of the nanoparticles formed were investigated. Typical SEM images of dewetted Au films of various thicknesses and their respective particle size distributions (PSD) are shown in Fig. 6. In brief, the mean particle size and the PSD width increase systematically with the nominal Au film thickness. On the other hand, increasing the annealing time is advantageous for “sufficiently thick” films, since it facilitates the formation of nanoparticles with smaller particle diameter and narrower PSDs compared to those annealed at shorter annealing times. In particular, for ultrathin Au films, i.e. $h \lesssim 3.5$ nm, spherical-like particles form, while annealing time does not seem to practically influence this morphology. For thicker Au films, i.e. $h \gtrsim 5$ nm, annealing at short times is not capable of bringing the Au particles to the morphology of the annealed thin films. However, increasing annealing time or annealing temperature improves appreciably the fragmentation of Au films to distributions with smaller particle diameter and width. Further, it was revealed that efficient and high throughput growth of ZnO nanowires, for a given growth time, was realized in cases of thin Au films, Fig. 7 (upper left), i.e. when the thickness is lower than 10 nm.

Figure 7 (bottom left) shows a FE-SEM magnification of the ZnO nanostructures grown on a 2 nm thick Au film dewetted at 900 °C for 30 s. ZnO nanorods (~100 nm) have initially grown from the substrate while thinner ones (~25 nm) protrude out of the thicker ones. This type of nanostructures implies a two-step growth mechanism. Images (b, c) of this panel were recorded with the backscatter electron (BSE) detector at 5 kV in Fig. 7(b) and 15 kV. Under these conditions, the ultrathin tips of the ZnO nanorods appear less clearly, while the bright spots represent the Au NPs. Similarly, image (d) shows an EDS mapping of the elements Au and Zn to support the existence of Au NPs dispersed in the ZnO nanostructures. These images demonstrate that, due to the abrupt growth conditions – since the Si/Au chip was placed at a preheated (900–950 °C) area of the tube and the growth lasted for ~2 min – Au nanoparticles first undergo coarsening to some extent and then act as catalytic sites for the growth of ZnO nanostructures. The coarsening of Au NPs might be responsible for the ZnO film which initially growth on Si as is evident from Fig. 7(a). However, since Au is now in contact with ZnO, the difference in wettability can cause further fragmentation of the bigger Au NPs to smaller ones. The latter could act as new nucleation sources for the growth of thinner ZnO nanowires. The above described mechanism is schematically illustrated in Fig. 7 (right panel) where possible steps of the growth process are shown. The different wettability of Au on ZnO structures is perhaps the key point for the observed behavior demonstrated in the schematic. The increased wettability of the catalyst droplet can lead to growth of nanowires of limited length. In this sense, the transition from step (c) to (d) in Fig. 7 (right panel) is decisive for controlling the formation of smaller Au NPs and their location on top of the already formed nanorods. As is evident from the SEM images, ultrathin tips can also grow at random positions, not only at the end of pre-existing nanorods, depending on the locations of small Au NPs. Finally, the ZnO NW arrays with the dispersed Au nanoparticles which remain on top of them after the growth process (Fig. 7; bottom left) could be used as substrates for surface enhanced Raman scattering, exploiting the plasmon properties of Au nanoparticles.

Solution chemistry growth of ZnO nanowires

The high temperature techniques for the controlled growth of ZnO NWs discussed above entail some disadvantages in the direction of integrating such NW arrays onto flexible organic substrates, which could lead to the fabrication of foldable devices. Several methods have been currently implemented for the growth of ZnO NWs in solutions [24]. ZnO can crystallize by the hydrolysis of Zn salts in a basic solution. As mentioned above, Zn^{2+} is tetrahedrally coordinated

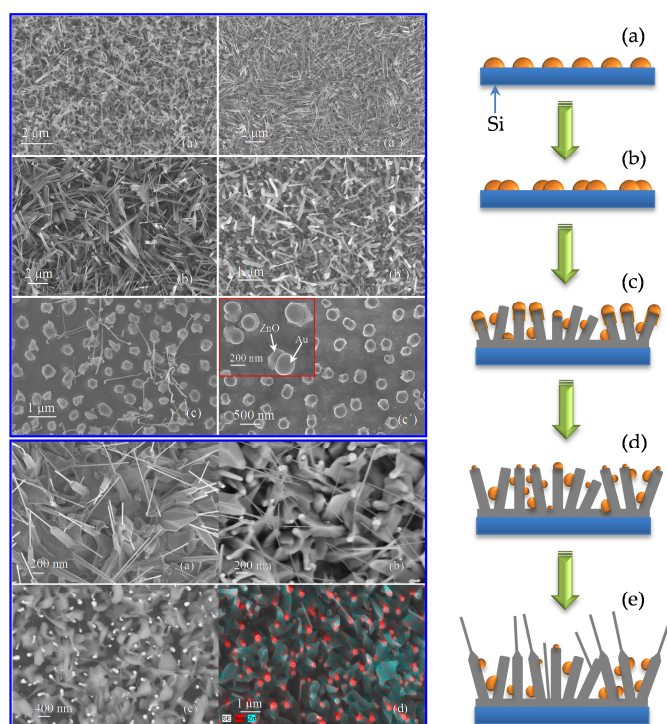


Figure 7. Upper Left: SEM images of ZnO nanostructures grown by VLS on Si substrates covered by Au films with thicknesses (a) 2 nm, (b) 5 nm, and (c) 15 nm. Bottom Left: (a) SEM magnification of the ZnO nanostructures shown in the upper left image (b). (b, c) Images of the same nanostructures recorded with the BSE detector at 5 kV (b) and 15 kV (c). (d) EDS mapping of the elements Au and Zn to support the existence of Au NPs dispersed in the ZnO nanostructures. These images demonstrate that, due to the abrupt growth conditions – since the Si/Au chip was placed at a preheated (900–950 °C) area of the tube and the growth lasted for ~2 min – Au nanoparticles first undergo coarsening to some extent and then act as catalytic sites for the growth of ZnO nanostructures. The coarsening of Au NPs might be responsible for the ZnO film which initially growth on Si as is evident from Fig. 7(a). However, since Au is now in contact with ZnO, the difference in wettability can cause further fragmentation of the bigger Au NPs to smaller ones. The latter could act as new nucleation sources for the growth of thinner ZnO nanowires. The above described mechanism is schematically illustrated in Fig. 7 (right panel) where possible steps of the growth process are shown. The different wettability of Au on ZnO structures is perhaps the key point for the observed behavior demonstrated in the schematic. The increased wettability of the catalyst droplet can lead to growth of nanowires of limited length. In this sense, the transition from step (c) to (d) in Fig. 7 (right panel) is decisive for controlling the formation of smaller Au NPs and their location on top of the already formed nanorods. As is evident from the SEM images, ultrathin tips can also grow at random positions, not only at the end of pre-existing nanorods, depending on the locations of small Au NPs. Finally, the ZnO NW arrays with the dispersed Au nanoparticles which remain on top of them after the growth process (Fig. 7; bottom left) could be used as substrates for surface enhanced Raman scattering, exploiting the plasmon properties of Au nanoparticles. Adapted with permission from Ref. [23].

forming the respective complexes. Solution temperature and pH determine the number of Zn^{2+} intermediates whose dehydration will finally lead to the formation of ZnO. The energy minimization of the reaction system is generally considered as the driving force for crystal growth, while a reversible equilibrium is considered to dictate the chemical reactions in an aqueous system. The high-energy polar surfaces (0001) have a high tendency to attract and adsorb the incoming ions, and alternating Zn and O terminated surfaces are formed during the reactions. This mechanism gives rise to anisotropic growth which leads to NW formation. Since solution chemistry growth takes place mostly in aqueous media, the term hydrothermal method is frequently used.

The growth of ZnO NWs has been achieved in alkaline solutions, in hexamethylenetetramine (HMTA) aqueous solution, by electrochemical deposition on conductive substrates, via templated growth in combination with electrodeposition, and by epitaxial growth where various metals such as Au, Pt, and Cu have been used as seeds on the substrate since they provide a lower lattice mismatch with ZnO [24]. The typical steps of the hydrothermal growth method of well-aligned ZnO NWs are illustrated in Fig. 8.

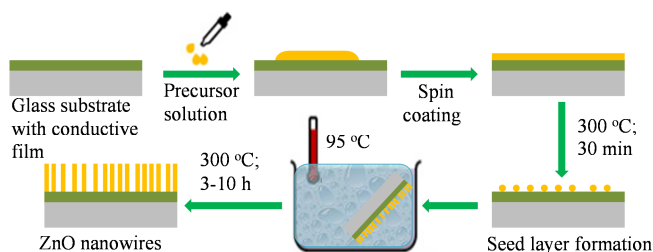


Figure 8. Schematic illustration of the various steps followed for the growth of ZnO NWs using the hydrothermal method.

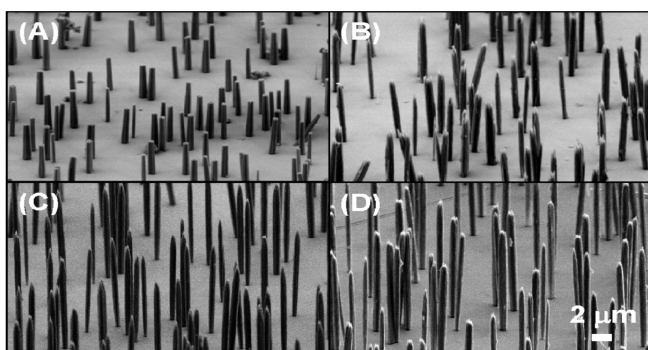


Figure 9. SEM images of ZnO NWs with aspect ratio of (A) 7.7, (B) 12.4, (C) 14.5, and (D) 22.3. Adapted with permission from Ref. [26], copyright (2009) American Chemical Society.

The seed layer can be formed by depositing ZnO nanoparticles onto the substrate. More frequently, droplets from a dispersion of a Zn-containing precursor (e.g. ZnAc dihydrate) are deposited by spin coating onto the substrate followed by thermal decomposition at >200 °C to form ZnO islands. The seeds facilitate nucleation of ZnO NWs due to lowering of thermodynamic barrier. An aqueous solution mixture of an alkaline reagent (e.g. HMTA or NaOH) and a Zn^{2+} precursor (e.g. ZnAc dihydrate, zinc nitrate etc.) is prepared as the nutrient solution. The solution may also contain a capping agent (e.g. polyethyleneimine, PEI) which prevents lateral growth of NWs to maximize their aspect ratio. The seeded substrate is kept (frequently face-down) into the solution over a certain period (e.g. 2 – 48 h) at constant temperatures (70 – 90 °C). Post-growth annealing (e.g. 300 °C for 30 min) takes place to remove organic matter from the ZnO NW surfaces. In analogy with the VLS method, a number of parameters involved in the hydrothermal growth of ZnO NWs must be properly optimized in order to obtain NW arrays with the desired morphology, i.e. orientation, areal density and aspect ratio. The reactants concentrations, the details of the seed layer, the growth time, the bath temperature, the position of the substrate, the solution pH, the present of capping agents, mechanical stirring, etc. are among the parameters that affect the morphology of ZnO NWs.

The density of ZnO NW arrays on smooth surfaces in the absence of seeds has been achieved by optimizing the precursor concentration [25]. Studying also the effect of growth time it was found that the growth process can be divided into three stages: (i) lateral growth, (ii) axial growth, and (iii) proportional growth. The optimum growth temperature was found to be 70 °C. In a more detailed study, Xu et al. [26] adopted a systematic statistical design and analysis to optimize the aspect ratio of ZnO NWs [26] (Fig. 9). Reaction temperature, growth time, precursor concentration and capping agent were the reaction parameters which were controlled. It was found that for precursor concentration ~ 1 mmol/L, at a reaction temperature ~ 80 °C, and growth time of about 30 h, the aspect ratio of the ZnO NWs achieved their highest value of nearly 23.

We have attempted in this article to provide a brief overview of the main advantages of 1D nanostructures and in particular of nanowires over other low-dimensional structures. NWs represent a class of nanomaterials the confinement of which in two dimensions (radially) can be exploited to benefit from changes in electronic and other physical properties, while, at the same time, their micron-sized long axis makes their manipulation for easy integration in opto-electronic and photonic devices possible. Thus, both their absolute size and their aspect ratio are important features. In addition, the geometry of NWs assists strain relaxation which in turn facilitates hetero-epitaxial growth even in the case of high lattice mismatch. A short description on the main applications and growth methods of ZnO NWs has been presented, where the pros and cons of the vapor deposition and solution chemistry synthesis approaches have been discussed. Both synthesis methods are multiparametric problems and fine tuning of the experimental parameters must be first conducted in order to achieve optimization of the NW growth, including location control, high aspect ratio and areal density, and vertical orientation to the substrate. Hierarchical or hybrid 1D nanostructures have also been developed to improve and provide tuning of the electrical and optical properties of NWs; considerable increase of the photovoltaic efficiency has been observed in hierarchically growth ZnO nanotree arrays.

REFERENCES

- [1] *Springer handbook of nanomaterials*, (Ed. Robert Vajtai), Springer, 2013.
- [2] X. Michalet, F. F. Pinaud, L. A. Bentolila, J. M. Tsay, S. Doose, J. J. Li, G. Sundaresan, A. M. Wu, S. S. Gambhir, S. Weiss, Quantum dots for live cells, in vivo imaging, and diagnostics, *Science* **307**, 538–544 (2005).
- [3] M. Yazawa, M. Koguchi, K. Hiruma, Heteroepitaxial ultrafine wire-like growth of InAs on GaAs substrates, *Appl. Phys. Lett.* **58**, 1080 (1991).
- [4] Y. Xia, P. Yang, Y. Sun, Y. Wu, B. Mayers, B. Gates, Y. Yin, F. Kim, H. Yan, One-dimensional nanostructures: Synthesis, characterization, and applications, *Adv. Mater.* **15**, 353–389 (2003).
- [5] S. H. Ko, D. Lee, H. W. Kang, K. H. Nam, J. Y. Yeo, S. J. Hong, C. P. Grigoropoulos, H. J. Sung, Nanoforest of hydrothermally grown hierarchical ZnO nanowires for a high efficiency dye-sensitized solar cell, *Nano Lett.* **11**, 666–671 (2011).
- [6] M. Law, L. E. Greene, J. C. Johnson, R. Saykally, P. D. Yang, Nanowire dye-sensitized solar cells, *Nat. Mater.* **4**, 455–459 (2005).
- [7] Z. L. Wang, ZnO nanowire and nanobelt platform for nanotechnology, *Mater. Sci. Eng. R* **64**, 33–71 (2009).
- [8] *Zinc oxide bulk, thin film and nanostructures*, (Eds. J Jagadish, S. J. Pearton), Elsevier, 2006.
- [9] Z. L. Wang, Nanostructures of zinc oxide, *Mater. Today* **7**, 26–33 (2004).
- [10] Z. Li, R. Yang, M. Yu, F. Bai, C. Li, Z. L. Wang, Cellular level biocompatibility and biosafety of ZnO nanowires, *J. Phys. Chem. C* **112**, 20114–20117 (2008).
- [11] P. D. Yang, C. M. Lieber, Nanorod-superconductor composites: A pathway to high critical current density materials, *Science* **273**, 1836–1840 (1996).
- [12] N. P. Dasgupta, J. Sun, C. Liu, S. Brittan, S. C. Andrews, J. Lim, H. Gao, R. Yan, P. Yang, 25th anniversary article: Semiconductor nanowires – synthesis, characterization, and applications, *Adv. Mater.* **26**, 2137–2184 (2014).
- [13] Z. W. Pan, Z. R. Dai, Z. L. Wang, Nanobelts of semiconducting oxides, *Science* **291**, 1947–1949 (2001).
- [14] M. H. Huang, S. Mao, H. Feick, H. Yan, Y. Wu, H. Kind, E. Weber, R. Russo, P. D. Yang, Room-temperature ultraviolet nanowire nanolasers, *Science* **292**, 1897–1899 (2001).
- [15] W. Z. Wu, Y. Wei, Z. L. Wang, Strain-gated piezotronic logic nanodevices, *Adv. Mater.* **22**, 4711–4715 (2010).
- [16] S. Xu, Y. Qin, C. Xu, Y. Wei, R. Yang, Z. L. Wang, Self-powered nanowire devices, *Nat. Nanotech.* **5**, 366–373 (2010).
- [17] B. Weintraub, Y. G. Wei, Z. L. Wang, Optical fiber/nanowire hybrid structures for efficient three-dimensional dye-sensitized solar cells, *Ang. Chem. Int. Ed.* **48**, 1–6 (2009).
- [18] Z. H. Zhang, X. Wang, J. B. Xu, S. Muller, C. Ronning, Q. Li, Evidence of intrinsic ferromagnetism in individual dilute magnetic semiconducting nanostructures, *Nature Nanotech.* **4**, 523–527 (2009).
- [19] R. S. Wagner, W. C. Ellis, Vapor-liquid-solid mechanism of single crystal growth, *Appl. Phys. Lett.* **4**, 89 (1964).
- [20] X. D. Wang, J. H. Song, P. Li, J. H. Ryou, R. D. Dupuis, C. J. Summers, Z. L. Wang, Growth of uniformly aligned ZnO nanowire heterojunction arrays on GaN, AlN, and $Al_{0.5}Ga_{0.5}N$ substrates, *J. Am. Chem. Soc.* **127**, 7920–7923 (2005).
- [21] J. H. Song, X. D. Wang, E. Riedo, Z. L. Wang, Systematic study on experimental conditions for large-scale growth of aligned ZnO nanowires on nitrides, *J. Phys. Chem. B* **109**, 9869–9872 (2005).
- [22] X. Wang, J. Song, C. J. Summers, J.-H. Ryou, P. Li, R. D. Dupuis, Z. L. Wang, Density-controlled growth of aligned ZnO nanowires sharing a common contact: A simple, low-cost, and mask-free technique for large-scale applications, *J. Phys. Chem. B* **110**, 7720–7724 (2006).
- [23] K. Govatsi, A. Chrissanthopoulos, V. Dracopoulos, S. N. Yannopoulos, The influence of Au film thickness and annealing conditions on the VLS-assisted growth of ZnO nanostructures, *Nanotechnology* **25**, 215601 (2014).
- [24] S. Xu, Z. L. Wang, One-dimensional ZnO nanostructures: Solution growth and functional properties, *Nano Res.* **4**, 1013–1098 (2011).
- [25] S. Xu, C. Lao, B. Weintraub, Z. L. Wang, Density-controlled growth of aligned ZnO nanowire arrays by seedless chemical approach on smooth surfaces, *J. Mater. Res.* **23**, 2072 (2008).
- [26] S. Xu, N. Adiga, S. Ba, T. Dasgupta, C. F. Jeff Wu, Z. L. Wang, Optimizing and improving the growth quality of ZnO nanowire arrays guided by statistical design of experiments, *ACS Nano* **7**, 1803–1812 (2009).